

# Photodegradation of Polyethylene: Factors Affecting Photostability

AYAKO TORIKAI, HAJIME SHIRAKAWA, SHIGEO NAGAYA,\* and  
KENJI FUEKI, *Department of Synthetic Chemistry, Faculty of Engineering,  
Nagoya University, Furo-cho, Chikusa-ku, Nagoya 464-01, Japan*

## Synopsis

Four kinds of annealed polyethylene (PE) films with varying densities were photo-irradiated with a medium pressure mercury lamp. Photodegradation processes were followed by ultraviolet (UV) and Fourier transform infrared (FTIR) spectroscopic techniques and by gel and mechanical property measurements. Oxygenated products build-up was more favored in linear low density (LLD) PE and the rate of formation increased in the reverse order of polymer density. A similar trend was seen in gel formation. Measurements of elongation at break (%) showed that the embrittlement time of photo-irradiated PE increased with the decrease of polymer density. The experimental results on unquenched samples were compared with those of quenched samples. It was found that the density (or crystallinity) and crystal size of PE play important roles in determining photostability.

## INTRODUCTION

A wide range of studies concerning photodegradation and photostabilization of polyethylene (PE) have been made recently.<sup>1,2</sup> Various factors affecting photostability of PE, such as light absorbing chromophores, effects of processing and morphology, have been examined. However, some controversy still remains. In our previous works,<sup>3,4</sup> we have studied the photodegradation of cross-linked PE and concluded that the photostability of PE probed by mechanical properties can be enhanced by crosslinking in spite of the fact that the rate of oxidation products formation is faster in the cross-linked PE. We have also studied the effect of polymer densities on the photodegradation of quenched PE.<sup>5</sup> Summarizing the results obtained from these studies, various factors seem to affect the photostability of PE.

In the present study, using annealed PE samples with varying polymer densities, we have investigated the role of tie molecules, which exist between crystalline lamellae in the photostabilization of PE.

## EXPERIMENTAL

Linear low density (LLD), medium density (MD), and two types of high density (HD) PE were supplied from Mitsui Petrochemical Industrial Co., Ltd. as pellets. The commercial name, density, melt index of the samples are listed

\* Plastic Laboratories, Showa Electric Wire and Cable Co., Ltd., Odasakae, Kawasaki-ku, Kawasaki 210, Kanagawa, Japan.

in Table I. PE films were prepared by hot-pressing for 10 min at 180°C and subsequently annealed to room temperature. The thickness of films are ca. 0.03 mm for FTIR measurements and ca. 0.08 mm for other measurements. Spectrograde n-hexane was supplied by Nakarai Chemicals Co., Ltd. and special grade ethanol and p-xylene by Kishida Chemicals Co., Ltd. They were used without further purification. The films were soaked in n-hexane overnight to remove impurities and then washed with ethanol before sample preparation.

Samples were photo-irradiated with a Toshiba H-400P medium pressure mercury lamp ( $\lambda \geq 250$  nm) in vacuum and in air at 30°C, and they were frequently turned over to give the same irradiation dose on both sides. The wavelength distribution of this lamp has been reported in our earlier paper.<sup>6</sup>

The photo-irradiated PE samples were stored in air or in vacuum for about one week for radical reactions to be completed,<sup>7</sup> and they were extracted with hot p-xylene by a Soxhlet extractor for 24 h and then dried under vacuum ( $10^{-4}$  mmHg) for overnight after washing with ethanol. The gel fraction (%) was estimated from eq. (1)

$$\text{Gel fraction (\%)} = (W/W_0) \times 100 \quad (1)$$

where  $W_0$  is the initial weight of polymers and  $W$  is the weight of fraction of photo-irradiated polymers insoluble in p-xylene. UV-visible and FTIR spectra of unirradiated or photo-irradiated samples were taken on a Hitachi 323 type spectrophotometer and a Nicolet MX-1 FTIR spectrophotometer, respectively. The tensile tests were carried out with a Shimadzu autograph using dumbbell type-2 samples (JIS K-6301). The elongation at break (%) was calculated from eq. (2)

$$\text{Elongation at break (\%)} = \frac{L - L_0}{L_0} \times 100 \quad (2)$$

where,  $L_0$  is the initial length of the samples and  $L$  is the elongated length attained at the break.

## RESULTS AND DISCUSSION

### Gel Formation in Photo-irradiated PE

The four samples were photo-irradiated in air and in vacuum at 30°C. After irradiations, the samples were allowed to stand for one week in air or in vacuum

TABLE I  
Characteristics of Polyethylene

Sample	Commercial name	Density (g/cm <sup>3</sup> )	Melt index (g/10 min)
I	Hizex 2200J (HD)	0.970	5
II	Hizex 5100B (HD)	0.945	0.25
III	Neozex 4060B (MD)	0.945	7
IV	Neozex 2015H (LLD)	0.922	1.2

to ensure completion of reactions of trapped radicals. The gel fraction (%) of samples I, II, III, and IV in air and in vacuum were determined from eq. (1). The amount of gel formed by the irradiation in vacuum increases in the order of sample I (HDPE) < sample II (HDPE) < sample III (MDPE) < sample IV (LLDPE). This result indicates that gel formation (crosslinking reaction) occurs predominantly in the amorphous region. When two samples have the same density (as II and III), the sample with a greater melt index gives a higher amount of gel formation. On photo-irradiation in air, the gel fraction increases in the reverse order: i.e., sample IV < sample III < sample II < sample I.

The result can easily be explained. In the presence of air, the competitive radical reactions leading to oxidation and crosslinking take place in the amorphous region. This explanation will be substantiated in a later section.

### Optical Absorption Measurements

#### *UV-Visible Spectra*

Changes in UV-visible spectra of PE photo-irradiated in air are shown for sample I in Figure 1. The absorption band having  $\lambda_{\max}$  at 245 nm which is attributed to diene structure<sup>8</sup> decreases gradually in intensity and new bands having  $\lambda_{\max}$  at 285 nm (triene), 324 nm (trienyl), 310 nm (tetraene), and 360 nm (tetraenyl)<sup>8</sup> appear and gradually increase in their intensities with the irradiation time. The strong absorption due to vinylene unsaturation having  $\lambda_{\max}$  at 185 nm also overlaps on shorter wavelengths of the spectra.

Similar spectral changes are observed in PE photo-irradiated in vacuum. Pentaenyl (394 nm) formation is also detected in the case of photo-irradiation

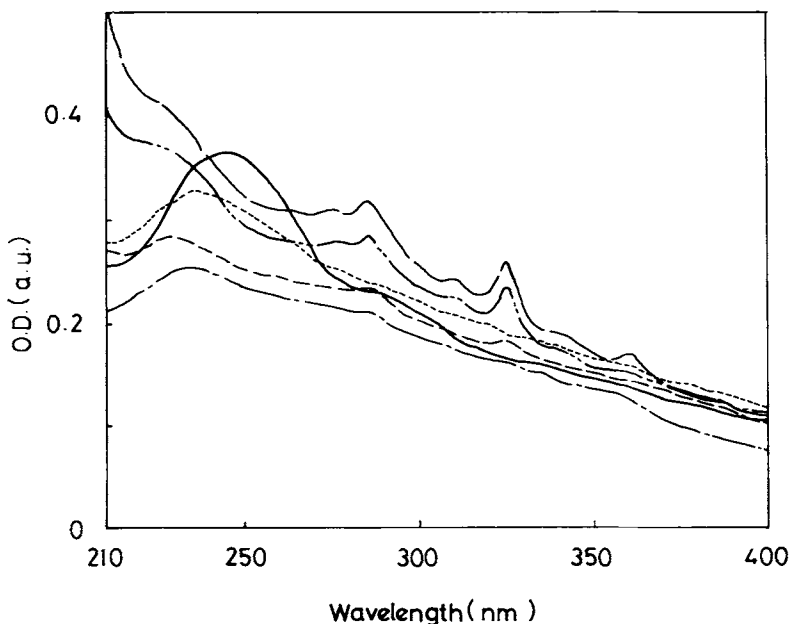


Fig. 1. Optical absorption spectra of photo-irradiated PE film (sample I) at 30°C in air: Irradiation time, —, 0 h; ----, 1 h; - · - · -, 3 h; ---, 5 h; - - - - -, 10 h; — — —, 15 h.

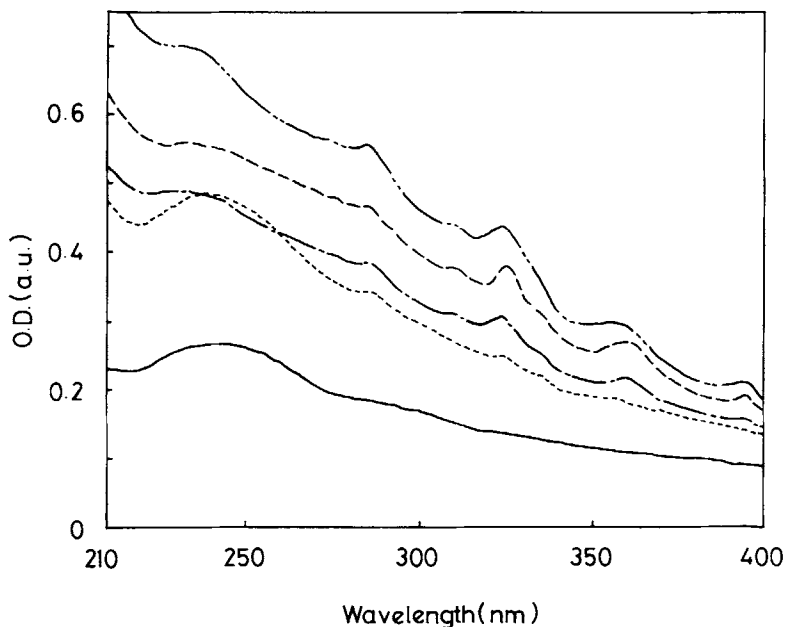


Fig. 2. Optical absorption spectra of photo-irradiated PE film (sample I) at 30°C in vacuum: Irradiation time, —, 0 h; ·····, 1 h; - - - - - , 3 h; - · - · - ·, 5 h; - - - - - , 10 h.

in vacuum as shown in Figure 2. These spectral changes are more clearly demonstrated for samples with higher densities. In other words, the sample having more crystalline regions forms the greater amounts of unsaturation. This result shows that the hydrogen abstraction reaction which results in formation of unsaturation takes place more favorably in the crystalline region of the polymer.

Photodegradation of PE may be initiated from photon absorption by diene structures, as shown in Figs. 1 and 2. The relative values of initial diene concentrations in four types of PE are estimated from UV-visible spectra and given in Table II. The initial diene concentration decreases in the order of sample I > sample II  $\approx$  sample III > sample IV: i.e., decreases with increasing amorphous fraction.

#### FTIR Spectra

Oxygenated products formation is monitored by the growth of  $1719\text{ cm}^{-1}$  ( $\nu\text{C=O}$ ) and  $3450\text{ cm}^{-1}$  ( $\nu\text{ROOH}$ ) in FTIR spectra.<sup>4</sup> The enlarged FTIR spectra in these two regions before and after photo-irradiation are given for sample IV in Figures 3 and 4. Various types of carbonyl formation (around 1700–1800

TABLE II  
Relative Concentration of Initial Diene Structure in PE

Sample	I	II	III	IV
Relative concn. (a.u.)	2.045	1.970	1.974	1.394

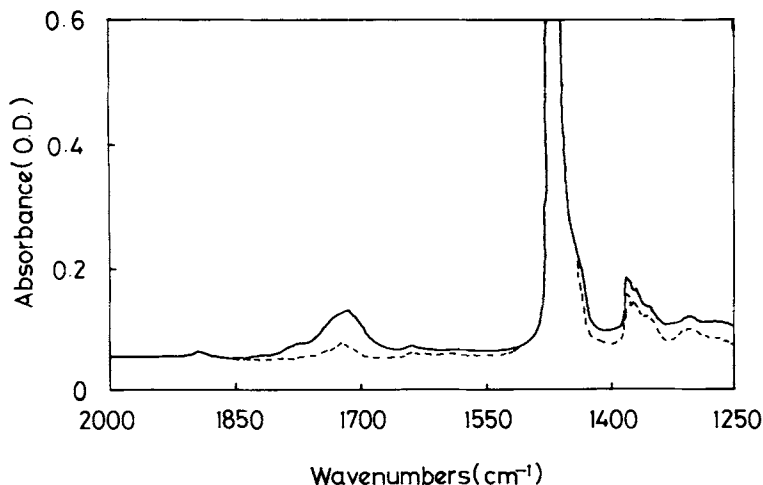


Fig. 3. Enlarged FTIR spectra in the carbonyl group region of PE (sample IV) photo-irradiated in air at 30°C: Irradiation time, ----, 0 h; —, 10 h.

$\text{cm}^{-1}$ ) and  $-\text{C}=\text{C}-$  bond formation (at  $1650 \text{ cm}^{-1}$ ) are found in Fig. 3. Hydroperoxide formation are also seen in Fig. 4.

Changes in the intensity of the  $\text{C}=\text{O}$  band at  $1719 \text{ cm}^{-1}$ , as represented by their OD/mm thickness, with irradiation time are shown in Figure 5. The optical density,  $\text{OD}_{1719}$ , increases in all four samples of polymer with an increase in irradiation time. This increase is most marked in sample IV (LLDPE). The rate of formation of carbonyl is the highest for sample IV (LLDPE) and least for sample I (HDPE). These results are in agreement with those of gel measurements (photo-irradiation in air) as mentioned in the previous section.

Similar results are also observed for the formation of OH group. As shown in Fig. 4, three peaks appear on photo-irradiation. For example, changes in the

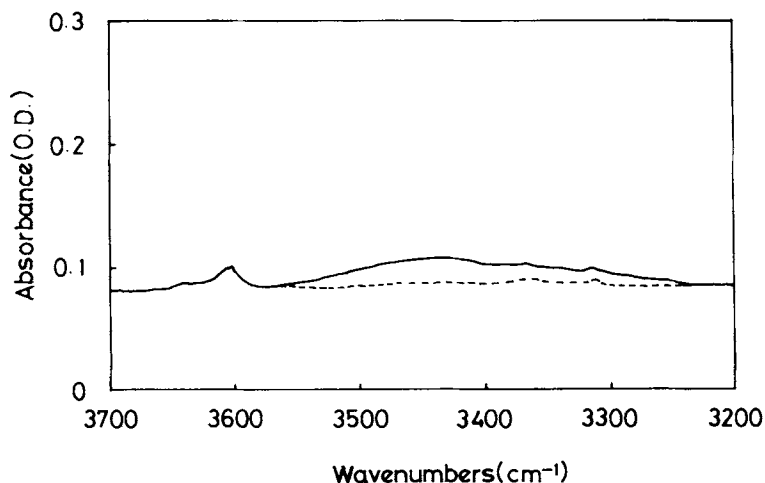


Fig. 4. Enlarged FTIR spectra in the hydroperoxide region of PE (sample IV) photo-irradiated in air at 30°C: Irradiation time, ----, 0 h; —, 10 h.

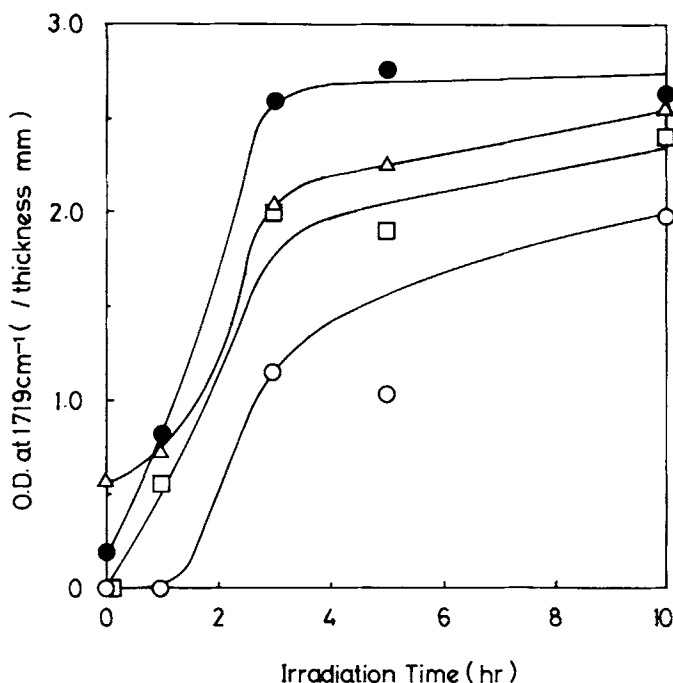


Fig. 5. Changes in optical density at  $1719\text{ cm}^{-1}$  with irradiation time of PE samples photo-irradiated in air at  $30^\circ\text{C}$ : sample I (○), II (△), III (□), and IV (●).

OD at  $3450\text{ cm}^{-1}$  ( $\text{OD}_{3450}$ ), as represented by their OD/mm thickness, with irradiation time are shown in Figure 6. Formation of OH group takes place more favorably in the order of sample I < sample II < sample III < sample IV.

Permeability (P) of PE to oxygen at  $25\text{--}30^\circ\text{C}$  was calculated by Rogers.<sup>9</sup> Some of these values are referred here and listed in Table III, where P is in the following units:

$$\frac{(\text{cm}^3 \text{ at STP})(\text{mm thickness}) \times 10^{10}}{(\text{cm}^2 \text{ area})(\text{S})(\text{cm Hg})}$$

It is clear that the permeability of PE films to oxygen parallel the rate of oxygenated products formation observed by FTIR spectra.

As mentioned earlier, the initial diene concentration of four samples decreases in the order of sample I > sample II  $\approx$  sample III > sample IV. This order is not parallel to the rate of oxygenated products formation. The photon absorbed by dienes may initiate photodegradation of PE and many other reactions than oxygenated products formation may occur; hydrogen abstraction to generate conjugated double bonds, crosslinking, and so on.

The initial  $\text{CH}_3$ -branch concentration of each sample was determined from a FTIR difference spectrum taking sample I as a standard. An example of the difference spectrum of methyl symmetrical deformation band is shown for sample IV in Figure 7. Details of calculating the  $\text{CH}_3$  concentration have been described in our previous paper.<sup>5</sup> The values estimated in this way are sum-

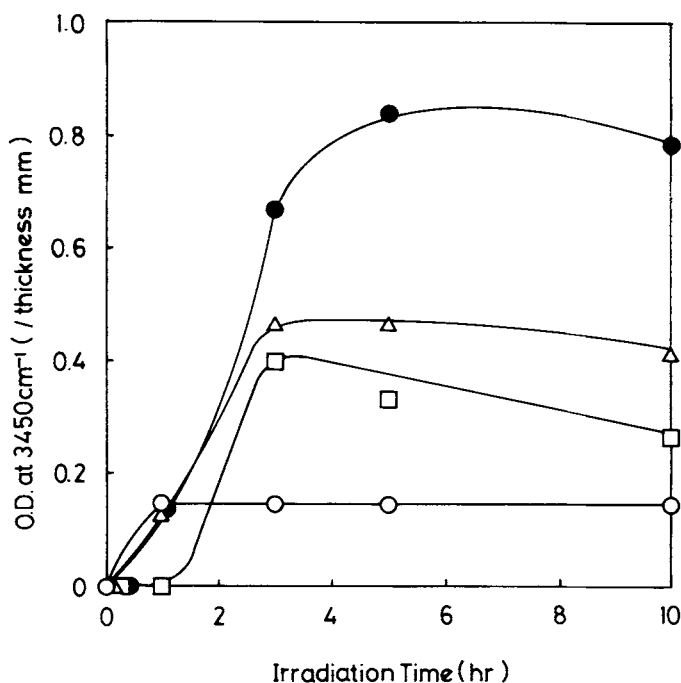


Fig. 6. Changes in optical density at  $3450\text{ cm}^{-1}$  with irradiation time of PE samples photo-irradiated in air at  $30^\circ\text{C}$ : Samples and symbols are the same as in Figure 5.

marized in Table IV. Samples having more  $\text{CH}_3$  branching give greater amounts of oxygenated products.

### Mechanical Properties

Measurement of mechanical properties, especially elongation at break, offers a means of direct estimation for polymer degradation. Changes in elongation at break (%) for each sample with irradiation time are shown in Figure 8.

Elongation at break (%) before photo-irradiation is the largest for sample IV (LLDPE) and decreases in the order of sample II > sample III > sample I. Sample IV is the most enduring to photo-irradiation as seen in Fig. 8 in spite of its higher degree of oxidation. Elongation at break of annealed HDPE is very small both before and after photo-irradiation.

The difference of elongation at break among four samples may be due to that of the density of PE. For example, samples having the greatest fraction of amorphous region such as LLDPE is the most stable against photo-irradiation.

TABLE III  
Permeability of PE Films to Oxygen at  $25\text{--}30^\circ\text{C}^9$

Density	0.965	0.938	0.922
P	0.5	21	55

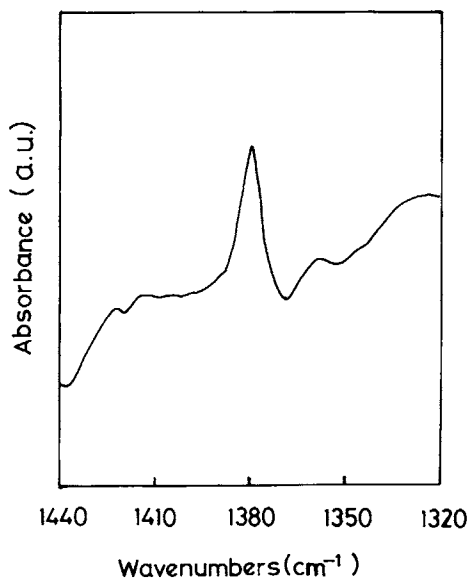


Fig. 7. FTIR difference spectrum of methyl symmetrical deformation band for sample IV. Reference: sample I.

tion. Photostability of PE cannot be evaluated by oxygenated products formation alone.

### Comparison with the Results for Quenched Samples

The conditions of film preparation may affect the photostability of PE as found in the case of  $\gamma$ -ray induced degradation of PE.<sup>10,11</sup> Annealed samples have larger crystallites than have quenched ones, even if the degree of crystallinity is equal, for both types of samples.

It has been reported that the crystal structure greatly affects the radiation-stability of polypropylene.<sup>12,13</sup> Quenched polypropylene (PP) is more resistant to  $\gamma$ -ray irradiation than is annealed PP. In the case of photo-irradiated PE, the initial elongation at break (%) of quenched samples is higher than that of annealed ones. In both types of samples, sample IV (LLDPE) shows the best photostability as evaluated by mechanical properties.

Photostability of LLDPE is better in quenched samples than in annealed ones. Any distinct difference between quenched samples and annealed ones was not found in this study except LLDPE, which is unlike  $\gamma$ -irradiated PP.

TABLE IV  
Initial CH<sub>3</sub>-branch Concentration of PE

Sample	I	II	III	IV
CH <sub>3</sub> /100C	0	0.718	0.371	2.260

These values were calculated from FTIR difference spectra taking sample I as a standard.



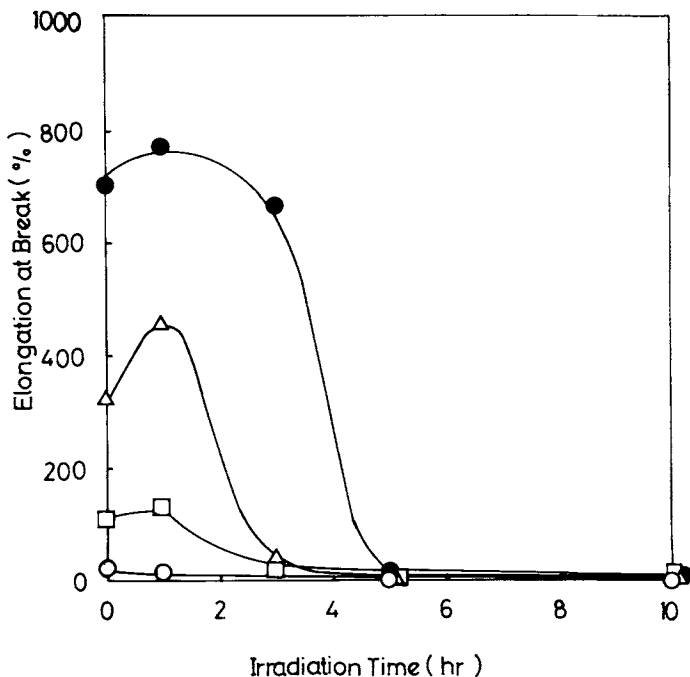


Fig. 8. Changes in elongation at break (%) with irradiation time of PE samples photo-irradiated in air at 30°C: Samples and symbols are the same as in Fig. 5.

However, elongation at break of quenched samples at a certain irradiation time is always greater than those of annealed ones.

### Factors Affecting Photostability

Although the oxygenated products formation more favors in the low density sample, such as LLDPE, photostability probed by a mechanical property (elongation at break) is greater in the low density sample. These results can be explained by invoking the existence of tie molecules between crystalline lamellae. Oxidation damage at the tie molecule region plays an important role in determining the embrittlement time. In HDPE, due to its highly crystalline nature, a small amount of oxidation products formation causes great damage in the tie molecules.

The photostability of quenched LLDPE (q-LLDPE) is superior to annealed LLDPE (a-LLDPE). Quenched PE has crystallites smaller than those of annealed PE. However, the degree of crystallinity did not depend upon the method of film preparation. Consequently, q-LLDPE has greater amounts of tie molecules and able to attain to higher oxidation products built-up without causing great damages in the tie molecules.

As already mentioned, there are various factors affecting photostability of PE. The density (or crystallinity) of PE and the size of crystallites were specifically discussed in this section as factors affecting photostability of PE.

We believe that it is significant in designing photostable polymers to explore various factors affecting photostability of polymers.

### References

1. A. Garton, D. J. Carlsson, and D. M. Wiles, in *Developments in Polymer Photochemistry-I*, N. S. Allen, Ed., Applied Science, London, 1980, p. 93.
2. D. M. Wiles and D. J. Carlsson, in *New Trends in the Photo-chemistry of Polymers*, N. S. Allen and J. F. Rabek, Eds., Elsevier Applied Science, London, 1985, p. 147.
3. A. Torikai, S. Asada, and K. Fueki, *Polym. Photochem.*, **7**, 1 (1986).
4. A. Torikai, A. Takeuchi, S. Nagaya, and K. Fueki, *Polym. Photochem.*, **7**, 279 (1986).
5. R. Geetha, A. Torikai, S. Nagaya, and K. Fueki, *Polym. Degradn. Stab.*, **19**, 279 (1987).
6. A. Torikai, T. Murata, and K. Fueki, *Polym. Photochem.*, **4**, 255 (1984).
7. T. Seguchi and N. Tamura, *J. Phys. Chem.*, **77**, 40 (1973).
8. D. C. Waterman and M. Dole, *J. Phys. Chem.*, **74**, 1906 (1970).
9. C. E. Rogers, in *Polymer Permeability*, J. Comyn, Ed., Elsevier Applied Science, London, 1986, p. 61.
10. A. Torikai, R. Geetha, S. Nagaya, and K. Fueki, *Polym. Degrad. Stab.*, **16**, 199 (1986).
11. R. Geetha, A. Torikai, S. Yoshida, S. Nagaya, H. Shirakawa, and K. Fueki, *Polym. Degrad. Stab.*, **23**, 91 (1988).
12. S. Nishimoto, *6th Kobunshi no Rekka to Anteika Kisakyoshitsu*, The Society of Polymer Science, Japan, 1986, p. 61.
13. S. Nishimoto, T. Kagiya, Y. Watanabe, and M. Kato, *Polym. Degrad. Stab.*, **14**, 199 (1986).

Received January 30, 1989

Accepted July 13, 1989